X-ray Crystal Structure Analysis of a Symmetrically Bridged Bishomocyclopropenyl Cation: 2,3-Dimethyl-7-phenyl-2-norbornen-7-ylium Hexafluoroantimonate(V)[1]

Thomas Laube

Contribution from the Laboratorium für Organische Chemie der Eidgenössischen Technischen Hochschule Zürich, ETH-Zentrum, Universitätstrasse 16, CH-8092 Zürich, Switzerland.
Received April 24, 1989

Abstract: The structure of the 2,3-dimethyl-7-phenyl-2-norbornen-7-yl cation (**7**) has been experimentally determined by X-ray structure analysis of **7**-SbF_6 and shows an unexpectedly strong bending of the C7 bridge toward the C2–C3 bridge with the double bond. The molecular structure is explained by the formation of a three-center, two-electron bond between C2, C3, and C7, as suggested by other authors in earlier works about similar cations. Simple energy estimations reveal that a benzylic, tertiary carbocation like **7** is strongly stabilized by such an interaction. A comparison of the experimental electron and difference density maps of **7** and the earlier published 1,2,4,7-*anti*-tetramethyl-2-norbornyl cation (**20**) with calculated maps excludes the possibility that the observed structures are space or time averages of ions with structures similar to those of corresponding neutral molecules, which do not show strong stereoelectronic effects. The crystal packing of **7**-SbF_6, **20**-Sb_2F_{11}, and several other published structures is analyzed in terms of cation–anion interactions, which may lead in solution to the formation of regioisomeric or diastereomeric solvolysis products. A correlation between the accessibility of a positively charged carbon atom to nucleophilic attack *in the crystal* with the observed solvolysis product ratios is found.

The 2-norbornen-7-yl or 7-norbornenyl ion (**1**) belongs to the most thoroughly investigated carbocations because of the extreme ratio of rates of solvolysis for the two diastereomeric precursors **2** and **3** (X = leaving group). In their pioneering work, Winstein

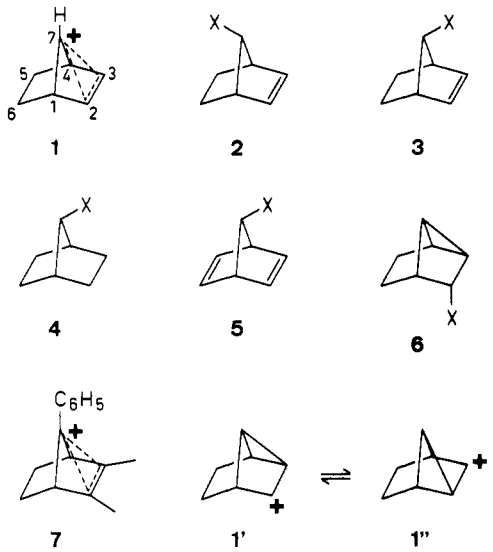

1 **2** **3** **4** **5** **6** **7** **1'** **1"**

et al.[2,3] and Roberts et al.[4] have shown that **2** (X = OTos) solvolyses 10^{11} times faster and **3** (X = OTos) 10^4 times faster than **4** (X = OTos). They explained this observation by assuming the formation of a nonclassical ion **1**, where the overlap between the C2=C3 double bond and the empty orbital at C7 leads to a charge delocalization. Such an intermediate explained also the stereoselective formation of the solvolysis product **2** (X = $OCOCH_3$)[2]. Even higher rates of solvolysis were observed for norbornadienyl derivatives (**5**) (leading to the norbornadienyl cation)[5,6] and *endo*-tricyclo[3.2.0.$0^{2,7}$]hept-6-yl derivatives (**6**)[7,8] (leading to **1**). The structure of **1** was controversially discussed, and it was proposed that **1** could actually be described as a pair of rapidly equilibrating tricyclic ions **1'** and **1"**.[9] Olah's[10] and Winstein's[11] NMR investigations of **1** and several substituted derivatives of **1** showed that even the 7-phenyl- and 2,3-dimethyl-7-norbornenyl cations are best represented by a symmetrically bridged cation of type **1**.[12] Recent ab initio investigations by Houriet[13] and Schleyer[14] also support the bridging in **1**. It is the aim of this work to find structural evidence for the bridging in the 2,3-dimethyl-7-phenyl-7-norbornenyl cation (**7**) by X-ray structure analysis of the salt **7**-SbF_6 and to compare some of its features with data from earlier published structures.

Synthesis and X-ray Structure Analysis

The synthesis started with the conversion of hexachlorocyclopentadiene (**8**) into the dimethylacetal **9**,[15] followed by a Diels–Alder reaction[16] with 1,4-dichloro-2-butene yielding **10** and HCl elimination with KOH[16] yielding **11** (Scheme I). Reduction with sodium and *tert*-butyl alcohol[17] gave the norbornadiene **12**, which was reduced[17] to the norbornene **13**. Cleavage of the acetal[18] yielded 2,3-dimethyl-2-norbornen-7-one (**14**), and the addition of phenyllithium[19] (in analogy to ref 20) gave a mixture of the diastereomers **15a** and **15b**, which were separated by flash

(1) For the first time presented in a short lecture at: Chemiedozententagung 1989, Bielefeld, West Germany, March 8, 1989.
(2) Winstein, S.; Shatavsky, M.; Norton, C.; Woodward, R. B. *J. Am. Chem. Soc.* **1955**, *77*, 4183–4184.
(3) Winstein, S.; Stafford, E. T. *J. Am. Chem. Soc.* **1957**, *79*, 505–506.
(4) Woods, W. G.; Carboni, R. A.; Roberts, J. D. *J. Am. Chem. Soc.* **1956**, *78*, 5653–5657.
(5) Story, P. R.; Saunders, M. *J. Am. Chem. Soc.* **1962**, *84*, 4876–4882.
(6) Winstein, S.; Ordronneau, C. *J. Am. Chem. Soc.* **1960**, *82*, 2084–2085.
(7) Tufariello, J. J.; Lorence, R. J. *J. Am. Chem. Soc.* **1969**, *91*, 1546–1548.
(8) Lhomme, J.; Diaz, A.; Winstein, S. *J. Am. Chem. Soc.* **1969**, *91*, 1548–1549.
(9) Brown, H. C.; Bell, H. M. *J. Am. Chem. Soc.* **1963**, *85*, 2324.
(10) Olah, G. A.; Liang, G. *J. Am. Chem. Soc.* **1975**, *97*, 6803–6806.
(11) Lustgarten, R. K.; Brookhart, M.; Winstein, S.; Gassman, P. G.; Patton, D. S.; Richey, H. G., Jr.; Nichols, J. D. *Tetrahedron Lett.* **1970**, 1699–1702.
(12) A wide variety of NMR investigations of 7-norbornenyl cations are described in: Metzger, B. Dissertation University of Karlsruhe (TH), Karlsruhe, West Germany, 1983 (Supervisor: Volz, H.).
(13) Houriet, R.; Schwitzguebel, T.; Carrupt, P.-A.; Vogel, P. *Tetrahedron Lett.* **1986**, *27*, 37–40.
(14) Bremer, M.; Schötz, K.; Schleyer, P. v. R.; Fleischer, U.; Schindler, M.; Kutzelnigg, W.; Koch, W.; Pulay, P. *Angew. Chem., Int. Ed. Engl.* **1989**, *28*, 1042.
(15) Newcomer, J. S.; McBee, E. T. *J. Am. Chem. Soc.* **1949**, *71*, 946–951.
(16) Hoch, P. E. *J. Org. Chem.* **1961**, *26*, 2066–2072.
(17) Gassman, P. G.; Aue, D. H.; Patton, D. S. *J. Am. Chem. Soc.* **1968**, *90*, 7271–7276. Gassman, P. G.; Patton, D. S. *J. Am. Chem. Soc.* **1969**, *91*, 2160–2162.
(18) Gassman, P. G.; Pape, P. G. *J. Org. Chem.* **1964**, *29*, 160–163.
(19) Seebach, D.; Neumann, H. *Chem. Ber.* **1974**, *107*, 847–853.

0002-7863/89/1511-9224$01.50/0

Table I. Selected Bond Lengths (Å), Angles (deg), and Torsion Angles (deg) of **7**

C1–C2	1.48 (1)	C1–C6	1.55 (1)	C1–C7	1.49 (1)
C2–C3	1.38 (1)	C2–C7	1.86 (1)	C2–C21	1.49 (1)
C3–C4	1.50 (1)	C3–C7	1.86 (1)	C3–C31	1.49 (1)
C4–C5	1.54 (1)	C4–C7	1.50 (1)	C5–C6	1.51 (1)
C7–C71	1.48 (1)				
C2–C1–C6	115.0 (6)	C2–C1–C7	77.1 (5)	C6–C1–C7	106.7 (6)
C1–C2–C3	108.4 (6)	C1–C2–C21	123.6 (7)	C3–C2–C21	125.3 (7)
C2–C3–C4	108.6 (6)	C2–C3–C31	124.5 (6)	C4–C3–C31	123.5 (6)
C3–C4–C5	115.1 (6)	C3–C4–C7	76.5 (5)	C5–C4–C7	106.8 (6)
C4–C5–C6	105.4 (6)	C1–C6–C5	105.3 (6)	C1–C7–C2	51.2 (4)
C1–C7–C3	87.1 (5)	C1–C7–C4	101.9 (6)	C1–C7–C71	129.4 (6)
C2–C7–C3	43.7 (3)	C2–C7–C4	87.6 (5)	C2–C7–C71	118.4 (5)
C3–C7–C4	51.6 (4)	C3–C7–C71	118.0 (5)	C4–C7–C71	128.4 (6)
C2–C1–C7–C71	−97.3 (5)	C1–C2–C3–C4	+0.1 (5)	C1–C2–C3–C31	+159.8 (7)
C21–C2–C3–C4	−161.7 (7)	C21–C2–C3–C31	−1.9 (8)	C3–C4–C7–C71	+97.9 (5)
C4–C5–C6–C1	+0.4 (5)	C1–C7–C71–C72	+164.0 (8)	C1–C7–C71–C76	−16.0 (8)
C4–C7–C71–C72	−9.0 (7)	C4–C7–C71–C76	+171.0 (8)		

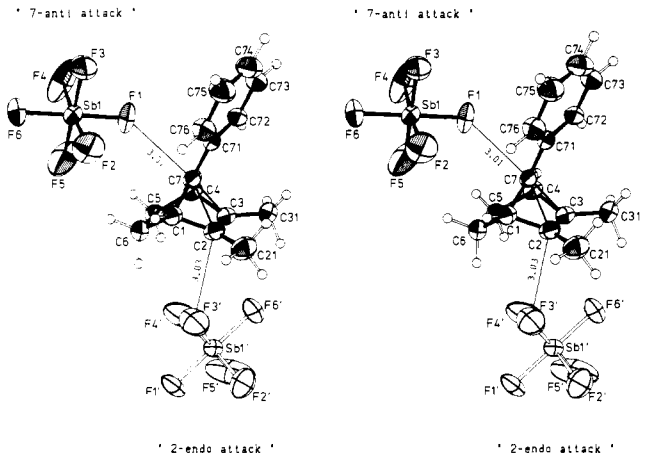

Figure 1. Stereo drawing (ORTEP) of the crystal structure of **7**-SbF_6. The counterion with the primed atom labels is generated by the symmetry operation $x - {}^1/_2, -y + {}^1/_2, z + {}^1/_2$ (distances in Å; the ellipsoids are drawn at the 50% probability level).

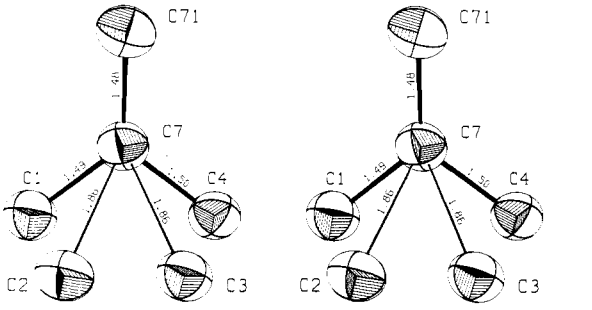

Figure 2. Stereo drawing (ORTEP) of the pentacoordinated carbon atom C7 and its bonding partners in the crystal structure of **7**. Only the bonds emanating from C7 are drawn (bond lengths in Å; the ellipsoids are drawn at the 50% probability level).

Table II. Distances and Angles between Least-Squares Planes ($P(i_1, ..., i_n)$ = Best Plane through $Ci_1, ..., Ci_n$) and Atoms, Bond Vectors, or other Planes in **7**

P(1,2,3,4)	C21	0.38 Å	P(1,3,21)	C2	0.14 Å
P(1,2,3,4)	C31	0.42 Å	P(2,4,31)	C3	0.15 Å
P(1,4,7)	C71	0.11 Å	P(1,4,71)	C7	0.04 Å
P(1,2,3)	C2–C21	14.8°	P(1,2,3,4)	P(1,4,7)	91.7°
P(2,3,4)	C3–C31	16.6°	P(1,4,7)	P(1,4,5,6)	144.6°
P(1,4,7)	C7–C71	4.3°	P(1,4,5,6)	P(1,2,3,4)	123.7°

chromatography and subsequent low-temperature recrystallization (their configuration as depicted in the formulas could be assigned with help of the data in ref 12). The 7-syn alcohol **15a** was converted into the chloride **16** (one diastereomer of unknown configuration) in analogy to a procedure of Coates.[21] Reaction with $SbCl_5$ gave upon recrystallization in CH_2Cl_2 the crystalline salt **7**-$SbCl_6$ from which the 7-anti alcohol **15b** could be obtained as the main product upon quenching with aqueous NaOH.[22] The chloride **16** was converted into the salt **7**-SbF_6 by reaction with silver hexafluoroantimonate and elimination of silver chloride. Recrystallization of **7**-SbF_6 from CH_2Cl_2 gave practically colorless crystals which were used for the X-ray structure analysis (see Experimental Section).

Figure 1 shows that the crystal consists of discrete cations **7** and anions SbF_6^-, neither of which exhibit crystallographic symmetry elements, but the cation has a local mirror plane in the norbornene cage within the given accuracy of the structure, and the anion has, as expected, an approximate octahedral symmetry. The most significant features of the structure are the short distances C2–C7 and C3–C7 (both 1.86 (1) Å) and the arrangement of the anions near to the atoms bearing the largest amounts of the positive charge. The mutual approach of C7 and the C2–C3 bridge in **7** leads to a 5-fold coordination of C7: it has three singly bonded partners (C1, C4, C71) and two weakly bonded partners[24] (C2, C3) as depicted in Figure 2. The phenyl ring is twisted by ca. 13° from the plane through C1, C4, and C7. The C2=C3 double bond (1.38 (1) Å) is significantly lengthened if compared with the standard value[25] of 1.331 Å for a normal tetraalkyl-substituted double bond. All other bond lengths have approximately the expected values (see Table I). In order to analyze the changes of the structure of the norbornene skeleton induced by the positive charge in **7**, the superposition of the cation with the calculated structure of 2,3-dimethyl-7-methylene-2-norbornene (**17**, $R = CH_3$) as the simplest model compound is shown in Figure 3. The strong deformation of the cation by the bending of the bridges can be expressed by the angles between the least-squares planes through the three bridges (see Table II). Remarkable also are the nonplanar coordination of C2, C3, and C7 (if one ignores the weak C2–C7 and C3–C7 bonds) and especially the *direction*

(20) Warkentin, J. *Can. J. Chem.* **1970**, *48*, 1391–1393.
(21) Coates, R. M.; Kirkpatrick, J. L. *J. Am. Chem. Soc.* **1970**, *92*, 4883–4892. Coates, R. M. Private communication.
(22) In the solvolysis product, no signals of the syn alcohol **15a** could be detected, but another product has also been formed (perhaps the tricyclic alcohol corresponding to **6**).
(23) The MM2(85) force field incorporated in MacroModel version 1.5 (Copyright 1987) was used. For MM2, see: Allinger, N. L. *J. Am. Chem. Soc.* **1977**, *99*, 8127–8134. MacroModel: Still, C. Columbia University, New York, NY 10027.
(24) An extrapolation with Pauling's empirical relationship between length and order of C–C bonds ($d_n = d_1 - 0.71$ Å log n; see: Pauling, L. *The Nature of the Chemical Bond and the Structure of Molecules and Crystals*; Cornell University Press: Ithaca, NY, 1960; Chapter 7-6) yields with $d_1 = 1.54$ Å a bond order of 0.36 for the C2–C7 and the C3–C7 bonds.
(25) Allen, F. H.; Kennard, O.; Watson, D. G.; Brammer, L.; Orpen, A. G.; Taylor, R. *J. Chem. Soc., Perkin Trans. 2* **1987**, S1–S19.

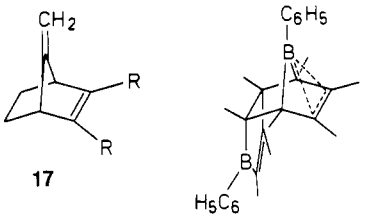

of the bending of the methyl groups with C21 and C31 into the exo half space of the C2=C3 double bond (in neutral norbornene derivatives, the C2 and C3 substituents are bent into the endo half space![26]). Also the C7–C71 bond is slightly bent into the syn half space of C7 (see Figure 3, bottom, and Table II). Simple steric interactions should result in a bending of C21 and C31 into the endo half space of the C2=C3 bridge and in a bending of C71 into the anti half space of the C7 bridge!

The packing in the crystal (see Figures 1 and 4) suggests approximately equal good interactions of **7** with the counterions in the 7-anti and the 2-endo positions, because the shortest $C^{\delta+}$···F distances are nearly equal (C7···F1 = 3.01 (1), C2···F3′ = 3.03 (1) Å).

Discussion of the Results

Structure of the Norbornenyl Cation (7). The short distances C2–C7 and C3–C7 and the lengthened double bond C2=C3 can be explained by an electronic interaction between the filled π orbital of the C2=C3 bond and the "empty" p orbital at C7 (which is simultaneously part of the conjugated benzyl cation). The result of this interaction is a delocalization of the positive charge about C2, C3, and C7 (and in the phenyl ring) and hence the formation of an aromatic bishomocyclopropenyl cation with a three-center, two-electron bond. The structure of the norbornenyl cage of **7** is practically identical[27] with that of the 7-bora-2-norbornenyl cage of **18**,[28] a fact that is in agreement with other analogies between boron compounds and carbocations.[29] In order to measure the overlap between the p-like orbitals at C2, C3, and C7, we have adjusted orthonormal s–p hybrid orbitals[30] on these atoms and calculated the Slater overlap integrals.[31] The results are shown in Figure 5 (left). This simple model does not explain the additional bending of the substituents with C21, C31, and C71 out of the planes of their bridges, because the cation **7** with planarized atoms C2, C3, and C7 (see Figure 5, right) has slightly higher overlap integrals. This failure, however, may be a result of our oversimplified electronic model. The same type of bending is observed in the structure of **18**, and the nonplanarity of C atoms in cyclopentadienyl rings of metallocenes was also explained in terms of a maximization of the overlap between carbon p orbitals and the metal atoms.[32] In order to estimate qualitatively the π resonance energy of the bishomoaromatic π system in **7** which must compensate the angle strain induced by the bending of the bridges, we have carried out some force-field calculations[23] on model systems (**17**, R = H or CH_3) and compared them with ab initio calculations on **1**.[13,14] The bending in **17**, R = H or CH_3 (both molecules behave very similarly in terms of the change in energy), was achieved by constrained energy min-

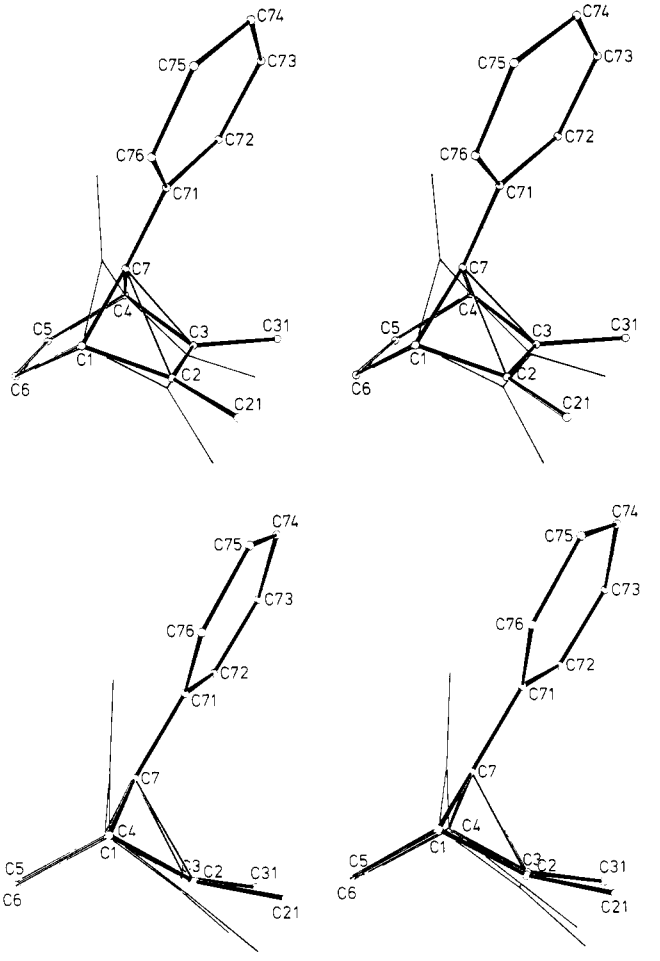

Figure 3. Two views (stereo drawings) of the superimposed skeletons of cation **7** (atoms drawn as spheres; bonds drawn as thick lines) and of 2,3-dimethyl-7-methylenenorbornene (**17**, R = CH_3; structure calculated by MM2(85);[23] bonds drawn as thin lines). The atoms C1, C4, C5, and C6 were adjusted with a 100-fold weighting compared with C2, C3, C7, C21, C31, and C71.

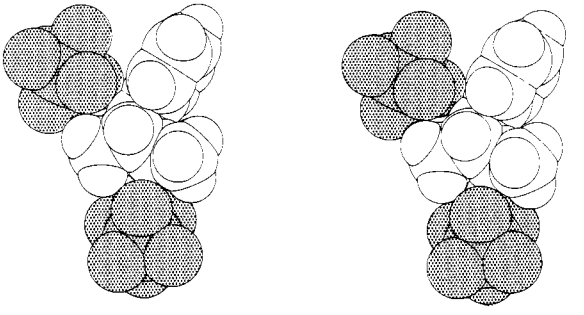

Figure 4. Stereo drawing of a space-filling model of **7** (white) and its nearest two counterions SbF_6^- (rastered; see Figure 1). The view direction is approximately along C1–C4 as in Figure 3 bottom. The atoms are represented by spheres with the corresponding van der Waals radii.

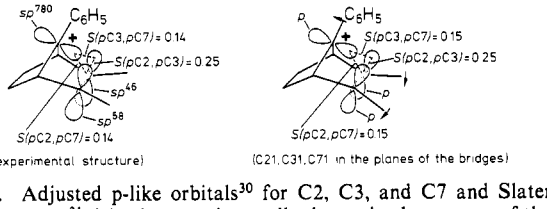

Figure 5. Adjusted p-like orbitals[30] for C2, C3, and C7 and Slater overlap integrals[31] S in the experimentally determined structure of the 7-norbornenyl cation **7** (left) and the corresponding structure where atoms C21, C31, and C71 were bent into the planes of their bridges (right).

(26) Pinkerton, A. A.; Schwarzenbach, D.; Birbaum, J.-L.; Carrupt, P.-A.; Schwager, L.; Vogel, P. *Helv. Chim. Acta* **1984**, *67*, 1136–1153. Houk, N. K. Methods in Stereochemical Analysis. In *Stereochemistry and Reactivity of Systems Containing π Electrons*; Watson, W. H., Ed.; Verlag Chemie International: Deerfield Beach, FL, 1983; Vol. 3, pp 1–40.

(27) Average deviation of the norbornene skeleton atoms C1 to C7 of **7** from the corresponding atoms of **18**: d_{av} = 0.05 Å (least-squares adjustment).

(28) Fagan, P. J.; Burns, E. G.; Calabrese, J. C. *J. Am. Chem. Soc.* **1988**, *110*, 2979–2981.

(29) Olah, G. A.; Prakash, G. K. S.; Williams, R. E.; Field, L. D.; Wade, K. *Hypercarbon Chemistry*; John Wiley & Sons: New York, 1987; pp 191–213.

(30) Haddon, R. C. *J. Am. Chem. Soc.* **1986**, *108*, 2837–2842.

(31) Mulliken, R. S.; Rieke, C. A.; Orloff, D.; Orloff, H. *J. Chem. Phys.* **1949**, *17*, 1248–1267. Preuss, H. *Integraltafeln zur Quantenchemie*; Springer-Verlag: Berlin, 1956; Vol. 1, pp 1–48.

(32) Dunitz, J. D.; Seiler, P. ETH Zürich, private communication.

Scheme I

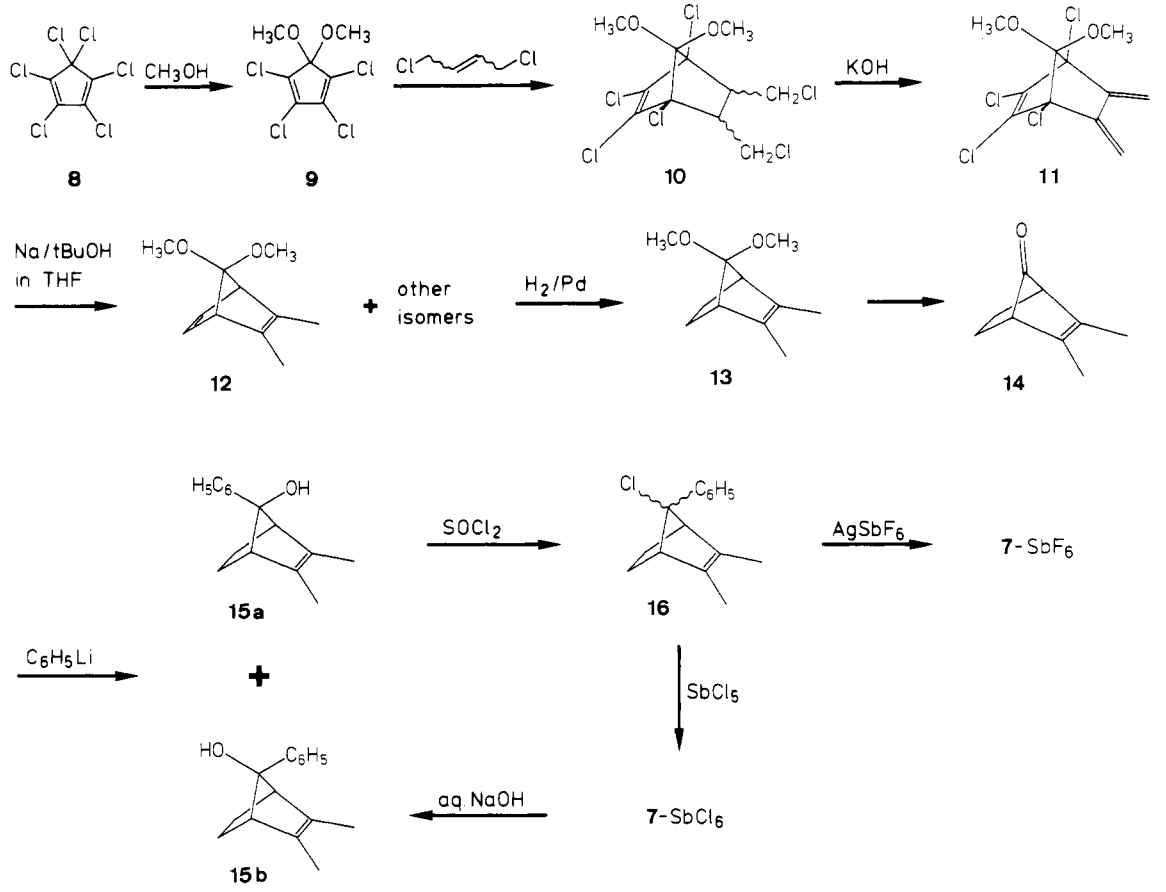

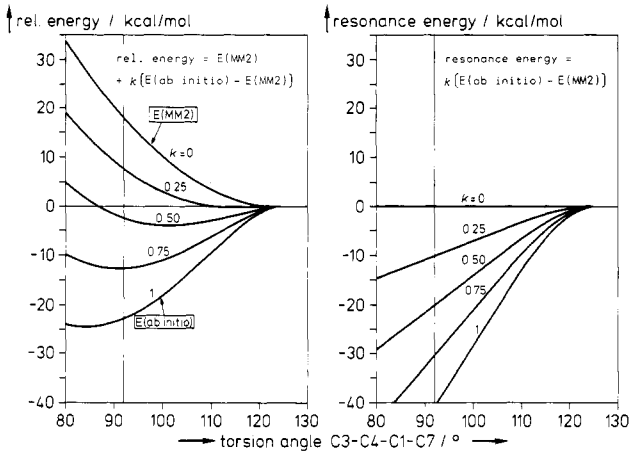

Figure 6. Qualitative estimation of the π resonance energy in 7-norbornenyl cations by comparison of the energy required for reducing the angle between the C2–C3 bridge and the C7 bridge in **17**, R = H or CH_3 (≡E(MM2)), with the energy required for widening this angle in cation **1**[13] (≡E(ab initio)) as functions of the torsion angle C3–C4–C1–C7. Left: simulation of the influence of increasing π resonance energy on the potential energy by continuous transformation of E(MM2) into E(ab initio) by variation of parameter k. Right: the resonance energy derived from the left diagram. The vertical line describes the experimental structure of **7**.

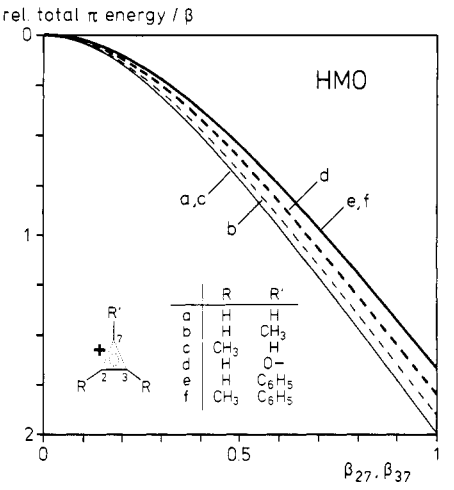

Figure 7. Relative total π energy (in β units) of substituted cyclopropenyl cations (numbering of the ring atoms as in 7-norbornenyl cations **1** and **7**) depending on the resonance integrals $\beta_{27} = \beta_{37}$ ($\beta_{23} = 1$ for all cases) according to the Hückel molecular orbital (HMO) theory.

imization,[33] subsequent removal of the penalty functions, and single-point energy calculation (see supplementary material). These models are used for the simulation of the bending *without* electronic interaction between the C2=C3 double bond and the empty orbital at C7.[34] The function, which describes the potential energy in **1** *with* electronic interaction, was constructed by fitting a polynomial to the data in ref 13 and slight extrapolation. Figure 6 shows that in a system without π resonance energy ($k = 0$) the torsion angle of 124° yields minimal energy. With increasing resonance energy ($k > 0$), the torsion angle of the structure with minimal potential energy is shifted toward 84° ($k = 1$, i.e., structure of **1**[13,14]). On the basis of this simple picture, the experimental structure of **7** (C3–C4–C1–C7 = +91.7 (6)°) may

(33) In different sets of calculations, either the C2–C7/C3–C7 distances or the C2–C1–C7/C3–C4–C7 angles or the C3–C4–C1–C7/C2–C1–C4–C7 torsion angles were constrained (i.e., the C_s symmetry was always retained). The results were similar in all cases.

(34) The force field[23] does not contain the parameters for a positively charged carbon atom. Because the models should have sp^2-like carbons at positions 2, 3, and 7, **17** with R = H or CH_3 are the nearest approximations of 7-norbornenyl cations.

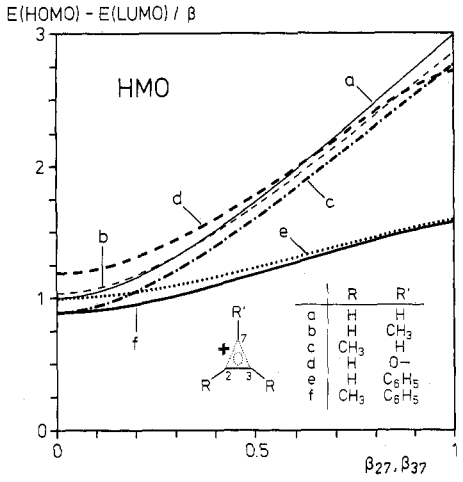

Figure 8. Energy difference between the highest occupied and the lowest unoccupied molecular orbitals (in β units) of substituted cyclopropenyl cations (numbering of the ring atoms as in **1** or **7**) depending on the resonance integrals $\beta_{27} = \beta_{37}$ ($\beta_{23} = 1$) according to the HMO theory.

be explained by assuming a π resonance energy of approximately three-quarters of that of the unsubstituted ion **1**: i.e., $k \approx 0.75$! Another independent and even more qualitative estimate of the π resonance energy may be obtained from the HMO theory (see Figure 7): in order to simulate different degrees of bridging, the resonance integrals $\beta_{27} = \beta_{37}$ were varied simultaneously. The highest resonance energy (i.e., lowest relative total π energy) is always obtained for case a in Figure 7 (corresponding to **1**), and the lowest resonance energy is always obtained for cases e and f (f corresponds to **7**). This is in agreement with the expectation because of the benzylic resonance in **7**, but the difference between the extreme cases, a and f, is relatively small. A rough estimation of β_{27} and β_{37} in **7** (or **1**) can be achieved with Mulliken's approximation[35] $\beta_{ij} = nS_{ij}$ (with n between 5 and 10): one obtains resonance energies between −15 and −35 kcal/mol for **7** and between −25 and −50 kcal/mol for **1** (assuming 1β unit = −20 kcal/mol[36]). Therefore, even the HMO theory predicts for cations like **7** a high stabilization upon forming the aromatic three-center, two-electron system. It should be mentioned here that the crystals of 7-SbF_6 were practically colorless, whereas benzyl cations are orange to red,[37] and this hypsochromic shift upon bridging is also qualitatively reproduced by the HMO theory (see Figure 8).

Considerations about Disorder in Carbocation Salts. The question of whether 7-norbornenyl cations are species with a single minimum (like **1**) or pairs of rapidly equilibrating ions[9,38] (like **1′** and **1″**; see Introduction), although already answered in favor of a single-minimum species by NMR[10,11] and solvolysis studies,[17] suggests an independent test. In the case of **7**, the corresponding pair of equilibrating ions **7′** and **7″** could also be present in the crystal, because the observed structure is the time average (over

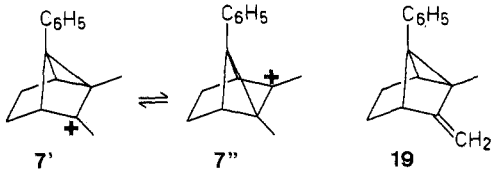

the time of the X-ray measurement) and the space average (over the whole crystal). Because the hypothetical structure of **7′** is not available to us, we assume that it has (in the extreme case of no electronic effects at all) practically the same structure as the neutral hydrocarbon **19**, which is the formal deprotonation product of **7′**. The structure of **19** was calculated by force-field methods, adjusted to its enantiomer (ent-**19**) by least-squares methods and drawn together with the averaged structure of both (see Figure 9). The phenyl ring was not included in the adjustment because it can freely rotate around the C7–C71 bond. The averaged structure in Figure 9 has a similar structure to **7** (omitting the phenyl ring): the maximal positional deviations between corresponding atoms are 0.11 Å for the norbornenyl cage

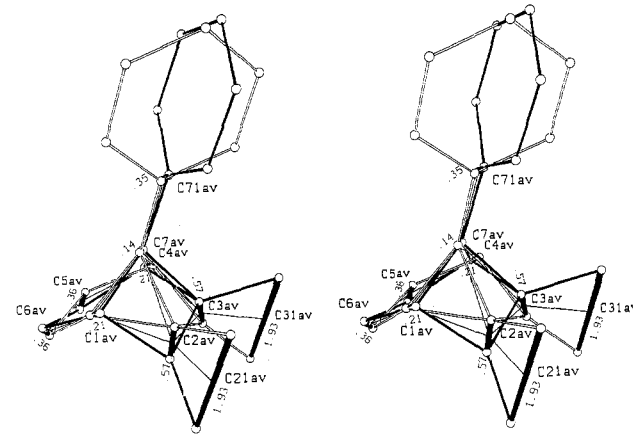

Figure 9. Stereo drawing of the superposition of 1-phenyl-7-methyl-6-methylenetricyclo[3.2.0.0^{2,7}]heptane (**19**) with its enantiomer (medium-thick black and white bonds; structure MM2(85)[23]). The structure generated by 1:1 averaging of corresponding atomic positions of the cage atoms C1–C7, the methyl, methylene, ipso, and para carbon atoms is represented by thin bonds and atom labels with the appendix "av" (the other phenyl ring atoms were not included in the adjustment). The lines connecting each pair of corresponding atoms in **19** and ent-**19** are represented by thick bars, and their lengths are given in angstroms.

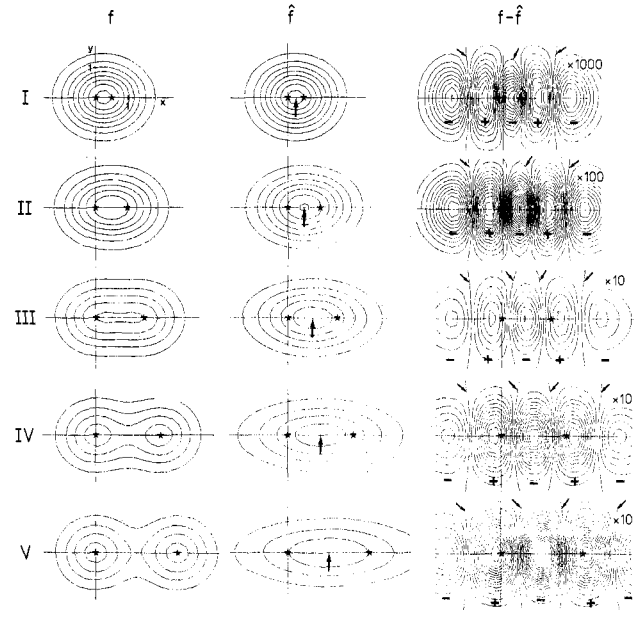

Figure 10. Adjustment[41] of three-dimensional anisotropic Gaussian density functions $\hat{f}$ (maximum: big arrows) on superpositions of two isotropic Gaussian density functions f (components: weights 0.5 and 0.5, maxima at ★, equal temperature factors) by minimization of $\int(f-\hat{f})^2\,dV$. The functions, f and $\hat{f}$, are normalized ($\int f\,dV = \int \hat{f}\,dV = 1$). The contour lines are drawn in a plane containing the symmetry axis (x) and have density distances of 0.02 for f and $\hat{f}$ and of 0.00002 (I) or 0.0002 (II) or 0.002 (III–V) for $f-\hat{f}$. The zero contours of $f-\hat{f}$ are marked by small arrows and the signs refer to the sign of $f-\hat{f}$. Distances of the maxima of the component functions of f (in length units) and $(\int(f-\hat{f})^2\,dV/\int f^2\,dV)^{0.5}$: I, 0.5, 0.2%; II, 1.0, 2.5%; III, 1.5, 10.4%; IV, 2.0, 23.6%; V, 2.5, 37.8%.

(35) Mulliken, R. S. *J. Phys. Chem.* **1952**, *56*, 295–311. See also: Scholz, M.; Köhler, H.-J. *Quantenchemie Ein Lehrgang*; Dr. Alfred Hüthig Verlag: Heidelberg, 1981; Vol. 3, pp 98–100, 184. Approximate values for S_{27}, S_{37} of the p-like orbitals: **1**, 0.17; **7**, 0.14; **17**, R = H or CH_3, 0.07.

(36) Heilbronner, E.; Bock, H. *Das HMO-Modell und seine Anwendung*; Verlag Chemie: Weinheim, 1970; Vol. 1, p 283.

(37) The 2,4,6-trimethylbenzyl cation has λ_{max} = 470 nm; see: Deno, N. C.; Jaruzelski, J. J.; Schriesheim, A. *J. Am. Chem. Soc.* **1955**, *77*, 3044–3051.

(38) Brown, H. C.; Schleyer, P. v. R. (comments) *The Nonclassical Ion Problem*; Plenum Press: New York, 1977; pp 59–66.

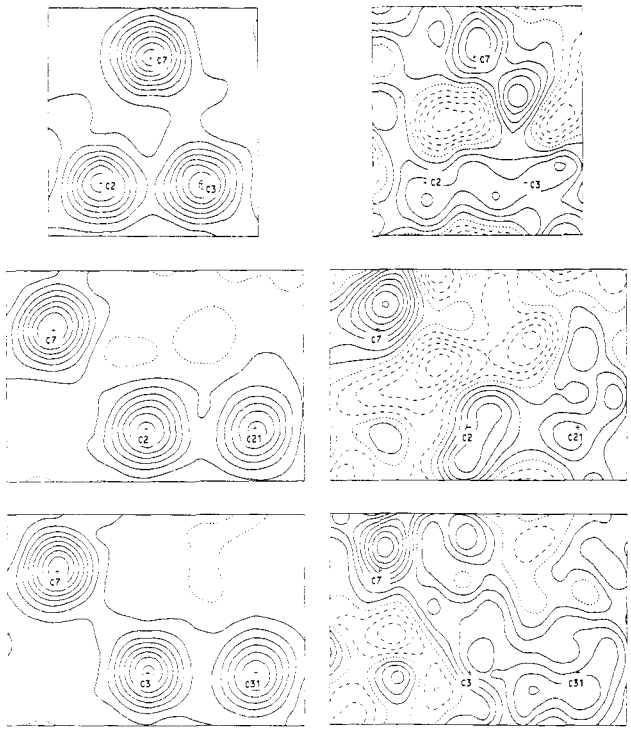

Figure 11. Electron density (left; F_{obs}; distances of the contour lines, 1 e/Å^3) and corresponding density (right; $F_{obs} - F_{calc}$; distances of the contour lines, 0.1 e/Å^3) maps of **7** (positive values, solid lines; negative, dashed; zero, dotted).

and 0.24 Å for C21, C31, and C71. However, the probability density functions (pdf's)[39] for the atoms in **7** should have their principal axes with the largest elongation approximately in the direction of the thick bars connecting corresponding atom positions[40] in Figure 9. This reasonable expectation has been verified by adjustment of three-dimensional anisotropic Gaussian density functions on superpositions of two isotropic Gaussian density functions in the least-squares sense[41] (see Figure 10). We ignore in this simple model the fact that the scattering density of an atom is the convolution of the electron density of a stationary atom with the pdf and identify f with the scattering density of a vibrating or disordered atom. Cases I–V in Figure 10 describe the influence of increasing distance between the two components in the density function (f) on the position of the center and the "thermal" parameters of $\hat{f}$. In all cases shown in Figure 10, the center of $\hat{f}$ is the arithmetic mean of the centers of the components of f, but if the distance between the maxima of the components of f becomes about 5 length units (lu), additional local minima for $\int (f - \hat{f})^2 \, dV$ appear if $\hat{f}$ has its center very near to the center of one of the components of f, and these local minima become (degenerate) global minima for distances of ca. 7 lu or more. The difference density maps ($f - \hat{f}$) and the measure for the goodness of fit ($(\int (f - \hat{f})^2 \, dV / \int f^2 \, dV)^{0.5}$) indicate the increasing discrepancy between f and $\hat{f}$ on going from I to V.

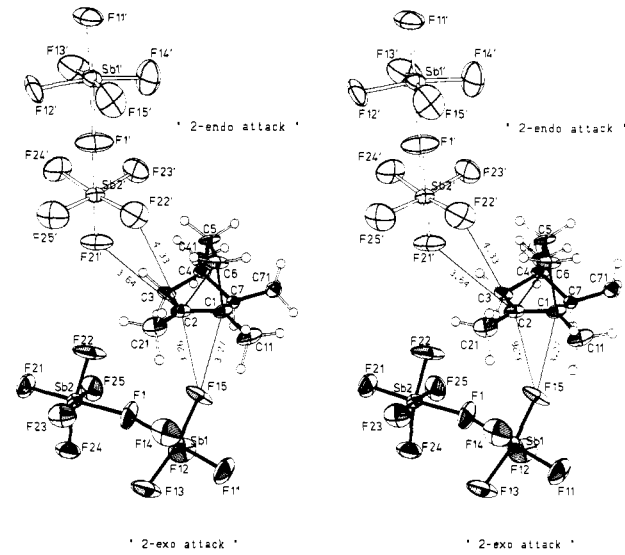

Figure 12. Stereo drawing (ORTEP) of the crystal structure of **20**-Sb_2F_{11} (data from ref 42). The counterion with the primed atom labels is generated by the symmetry operation $-x + 1$, $y - {}^1/_2$, $-z + {}^3/_2$ (distances[43] in angstroms; the ellipsoids are drawn at the 50% probability level).

From Figure 9 one would expect for C21av and C31av separated positions each with a half-population because of the 1.93-Å distance between the positions. The ORTEP drawing of **7** in Figure 1 shows that the cage atoms and C21, C31, and C71 have practically isotropic pdf's! Therefore, we can exclude the assumed disorder between the extreme structures **7'** and **7''** on the basis of the pdf's of C21 and C31 (but not on the basis of the positions of the atoms). In addition to this analysis, we have examined the electron density (F_{obs}) and difference density ($F_{obs} - F_{calc}$) maps of **7** in the critical region around C2, C3, and C7 (see Figure 11). A visual comparison of the density functions (f) in Figure 10 with the electron density (F_{obs}) maps in Figure 11 (left) suggests that 2 lu in Figure 10 corresponds roughly to 1 Å in Figure 11. The shape of the electron density contour lines of all atoms in Figure 11 is comparable at worst with the contour lines of f in case I of Figure 10, and from this it follows that hidden disordered positions could have only a maximal distance of ca. 0.25 Å (f and $\hat{f}$ in cases II–V are too anisotropic to be comparable with the experimental electron densities). Therefore, the assumed disorder between **7'** and **7''** can also be excluded on the basis of the electron densities (F_{obs}) of C2 and C3. The low crystallographic quality of the structure of **7**-SbF_6 is reflected by the noisy difference density maps (Figure 11, right) and rules out any search for bond densities. A systematic error in F_{calc} (resulting from an erroneous although refined scale factor; see Experimental Section) yields positive difference densities for all atoms, but besides this artifact, one cannot find hints for hidden disordered positions of C21 or C31. The large distance between the hypothetical disordered positions of these atoms would result in wide negative peaks in the difference density maps of Figure 11 (right) with their minima at the positions of C21 and C31 and in positive peaks with their maxima near the true positions (approximately like case V in Figure 10, if the $f - \hat{f}$ map was stretched along the x axis). For the cage atoms of **7**, the expected separations of the disordered positions (Figure 9) would correspond to case I or II in Figure 10, but in these cases, the expected difference densities are far too small to

(39) See, for example: Willis, B. T. M.; Pryor, A. W. *Thermal Vibrations in Crystallography*; Cambridge University Press: London, 1975; pp 92–95.

(40) Dunitz, J. D.; Schomaker, V.; Trueblood, K. N. *J. Phys. Chem.* **1988**, *92*, 856–867. Dunitz, J. D.; Maverick, E. F.; Trueblood, K. N. *Angew. Chem., Int. Ed. Engl.* **1988**, *27*, 880–895.

(41) According to Plancherel's equation (corresponds to Parseval's theorem), the adjustment in the direct space corresponds to an adjustment in the reciprocal space: $\int_{-\infty}^{\infty} |f(x)|^2 \, dx = \int_{-\infty}^{\infty} |F(s)|^2 \, ds$, where $F(s)$ is the Fourier transform of $f(x)$. See textbooks about Fourier analysis, for example: Zygmund, A. *Trigonometric Series*, 2nd ed.; Vol. I and II combined; Cambridge University Press: Cambridge, 1988; Vol. II, pp 248–250. Champeney, D. C. *A handbook of Fourier theorems*; Cambridge University Press: Cambridge, 1987; pp 54, 71–74. For all integrals ($\int g \, dV \equiv \int_{-\infty}^{\infty} \int_{-\infty}^{\infty} \int_{-\infty}^{\infty} g \, dx \, dy \, dz$, where g is any of the integrands used here), analytical formulas have been derived (MACSYMA, Massachusetts Institute of Technology, 1982; Symbolics, Inc., 1988) from which the optimal parameters for $\hat{f}$ were determined by nonlinear optimization (the symmetry of f reduces the number of parameters to be determined for $\hat{f}$ from nine to three: one positional and two thermal parameters). The components of f always have the form $\exp(-(\mathbf{x} - \mathbf{x}_0)^T(\mathbf{x} - \mathbf{x}_0))$ with $\mathbf{x}, \mathbf{x}_0 \in \mathbf{R}^3$ (omitting the normalizing and weight factors). An important difference between the theoretical f or $f - \hat{f}$ maps if compared with the electron or difference density map of an X-ray structure results from the phase information of their Fourier transforms. For f we used the "true" phase angle function and obtain an exact f map. For electron density maps, the phase angles of the adjusted structure are used as a good approximation of the unknown "true" phase angles. Theoretical maps where the amplitude of f and the phase angle of $\hat{f}$ were combined (using numerical integration) are similar to the f and the corresponding $f - \hat{f}$ maps in cases I and II but deviate strongly for cases IV and V because of the bad overall agreements (much worse than the experimental R values).

be recognizable in the experimental difference density maps in Figure 11.

Resuming all results, one can say that the experimental data for **7** contain no hints for hidden disorder in the sense of a superposition of **7′** and **7″** according to Figure 9 on the basis of electron or difference density map. However, if **7′** and **7″** are much more similar to **7** with regard to their structure (and energy) so that all distances between corresponding disordered positions are in the range of a few tenths of an angstrom, then it becomes impossible to detect such a disorder because it is not distinguishable from the thermal motion[40] (root of the mean-square amplitude of atoms in organic crystals: 0.1–0.3 Å) of a single atom.

A similar situation was found in the crystal structure of the 1,2,4,7-*anti*-tetramethyl-2-norbornyl cation[42] (**20**; see Figure 12):

20 **21** **22**

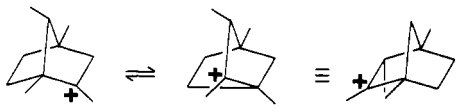

20′ **20″**

is it possible that the experimentally determined structure of **20** is actually a superposition of the two classical[44] Wagner–Meerwein isomers **20′** and **20″** (with approximate weights 0.75 and 0.25)? Because the classical[44] structures of **20′** and **20″** are not available to us, we assumed that they might have the same structure as hydrocarbons **21** and **22**, which are the formal deprotonation products of **20′** and **20″**. The 3:1 average is shown in Figure 13 (approximately the same view as for **20** in Figure 12). The largest distance between corresponding positions is 0.95 Å for C6av, whereas distances of ca. 0.6 Å are found for C1av, C2av, C11av, and C21av. In order to estimate the expected shape of the electron and difference density functions of **20** in the case of a disorder as described in Figure 13, we have adjusted three-dimensional anisotropic Gaussian density functions ($\hat{f}$) on superpositions of two isotropic Gaussian density functions with weights 0.75 and 0.25 (because of the 3:1 disorder model) and different distances (these functions correspond to electron density functions as in the foregoing case). The results are shown as contour line diagrams in Figure 14. As in the case of a 1:1 disorder model (Figure 10), the principal axis with the largest elongation of $\hat{f}$ coincides with the line connecting the two centers of the disordered positions, but the center of $\hat{f}$ is always closer to the peak with the higher weight than the arithmetic mean of the two centers. For large distances between the two centers, the center of $\hat{f}$ approaches the center of the peak with the higher weight (they coincide in the limit of infinite distance!), and the smaller peak of $\hat{f}$ looses its influence on $\hat{f}$ but becomes clearly detectable in the difference density map! From Figure 13, one would expect that the thermal ellipsoids for C1, C2, C11, and C21 have their axes with the largest elongation approximately in a vertical direction, whereas the ORTEP diagram (Figure 12) shows that these axes have horizontal directions for C1, C2, and C11, and this is a contradiction to the proposed disorder model. For C6, the predicted and the experimentally determined axes have the same direction. The electron density maps for the region about C1, C2, and C6 in **20** (Figure 15, left) show that, also in this case, 2 lu in Figure 14 corresponds roughly to 1 Å. Therefore, the electron density contour lines for C1, C2, C11, and C21 should have shapes like those for $\hat{f}$ in Figure 14, case II or III (which correspond to distances of 0.5 or 0.75 Å between the disordered positions), and for C6, one would expect contours like those for $\hat{f}$, case IV (corresponding to a distance of 1 Å).[45] The experimental electron density maps in Figure 15 do not show significant similarity with case III or IV of $\hat{f}$ in Figure 14, and case II may be excluded on the basis of the direction of the largest elongation of the pdf's. The difference density maps of **20** (Figure 15, right) have a very wavy background[46] (the positive and negative peaks have absolute maxima up to 1 e/Å^3), but the high peak near C2 lies approximately in the expected position according to the less populated orientation in Figure 13. The corresponding peak for C1, however, could not be found, only a weak second peak for C6 is detectable near the expected position, but if compared with the noise, they are not significant. The peak near C2 does not lie near the principal axis of the largest elongation of the pdf and may result as well from an anharmonic potential of the vibration of C2 along the reaction coordinate of the Wagner–Meerwein rearrangement. The pdf for C6 in Figure 12 suggests that C6 may vibrate with large amplitudes in that direction.[47] Resuming all arguments, one can say also that in the structure of **20** there are no hints of a hidden disorder that is so severe that it would cause significant changes of the geometry of **20**.

Analysis of the Crystal Packing and Comparison with Other Structures. The crystal packing of **7**-SbF_6 reveals an interesting aspect: cation **7** is in the closest neighborhood surrounded by two anions (see Figure 1) that have practically identical shortest $C^{\delta+}\cdots F$ distances (3.03 and 3.01 Å) and that seem to fit equally well on the van der Waals surface of **7** (Figure 4). We suggest that this fact may indicate comparably easy attack of nucleophiles on cation **7** in solution, leading to products of type **2** in the case of a 7-anti attack and of type **6** in the case of a 2-endo attack (X^- = nucleophile).[48] If the nucleophilic attack on 7-norbornenyl cations in solution is kinetically controlled, one would expect comparable amounts of the regioisomers of type **2** and **6**! Solvolysis studies[2] have shown that **2** (X = OTos) yields exclusively **2** (X = OAc), whereas **3** (X = OTos) gives, due to a Wagner–Meerwein rearrangement or 1,6-σ participation,[3] 2-bicyclo[3.2.0]hepten-4-ol. Higher substituted derivatives of **2** or **3** with *p*-anisyl groups at C7 gave upon solvolysis mixtures of products[49] corresponding to **2** and **3** in the ratio of ca. 15:1. When $NaBH_4$ or $LiAlH_4$ were used as the trapping reagent[9,50] in the solvolysis of **2** (X = OTos), the tricyclic product **6** (X = H) was obtained as one of the main products. It should be noted that the high thermodynamic instability of **6** (X = OH) if compared with **2** or **3** (X = OH) could be demonstrated by equilibration[51] to give exclusively **2** (X = OH). Considering the arrangement of the counterions around **7** in the crystal (Figures 1 and 4), one would expect that solvolysis products of type **2** and **6** are formed, although 7-norbornenyl ions like **7** are *not* pairs of equilibrating ions **7′** and **7″**. The fact that the solvolysis products of type **6** were hardly observed or isolated may

(42) Laube, T. *Angew. Chem., Int. Ed. Engl.* **1987**, *26*, 560–562.

(43) The unsignificant differences between the positional and thermal parameters of **20**-Sb_2F_{11} as published,[42] and those used here are due to technical problems (revival of the data under a different operating system).

(44) "Classical" is used here in the sense of complete absence of electronic effects like σ participation, which means that the structure of the ion is similar to that of a comparable neutral molecule (for example, a hydrocarbon).

(45) For a carefully examined example of static disorder with similar distances between corresponding positions see: Siegel, J.; Gutiérrez, A.; Schweizer, W. B.; Ermer, O.; Mislow, K. *J. Am. Chem. Soc.* **1986**, *108*, 1569–1575.

(46) It should be noted here that the highest maxima in the electron density maps are about 120 e/Å^3 at the two Sb atoms and that several experimental difficulties occurred during the measurements (see ref 42, footnote 11).

(47) Unfortunately, it seems to be very difficult to differentiate in crystal structures with an accuracy like that of **20**-Sb_2F_{11} between disorder models with small distances between the disordered positions and thermal motion with anharmonic potentials. We calculated density functions ($\hat{f}$) and difference density functions ($f-\hat{f}$) for several simple anharmonic vibrations, and they were practically undistinguishable from those depicted in cases I–III of Figure 14.

(48) This consideration is related to the work of Bürgi and Dunitz about the nucleophilic attack on carbonyl compounds, which may be considered as highly stabilized carbocations; see: Bürgi, H. B.; Dunitz, J. D.; Shefter, E. *Acta Crystallogr., Sect B* **1974**, *B30*, 1517–1527.

(49) Gassman, P. G.; Zeller, J.; Lumb, J. T. *J. Chem. Soc., Chem. Commun.* **1968**, 69–71.

(50) Winstein, S.; Lewin, A. H.; Pande, K. C. *J. Am. Chem. Soc.* **1963**, *85*, 2324–2326.

(51) Tufariello, J. J.; Mich, T. F.; Lorence, R. J. *J. Chem. Soc., Chem. Commun.* **1967**, 1202–1203.

be a consequence of equilibration under acidic conditions (i.e., thermodynamic control). The attack of nucleophiles X^- to give 7-syn or 2-exo products is hardly observed during solvolyses, and in our crystal structure, no counterion is arranged in positions suitable for a 7-syn or a 2-exo attack (the nearest counterion at the three-center, two-electron bond is found in front of the methyl groups with C21 and C31, but with the Sb atom practically in the plane of C1, C2, C3, and C4). Figure 4 shows that there is no place for good van der Waals and electrostatic interactions in the 7-syn/2-exo region of **7**!

Similar correlations between arrangements of anions around carbocations and product ratios upon solvolyses of similar cations were also observed in other cases. Another striking example[42,52] is the norbornyl cation **20**: the two nearest $Sb_2F_{11}^-$ counterions seem to attack with one F atom the exo side and the endo side of C2, which is assumed to bear the largest amount of the positive charge (see Figure 12). The 2-exo attack of F15 on C2 (or C1, which would lead to the "Wagner–Meerwein isomer") seems to be possible practically along the symmetry axis of the "empty" p orbital of C2 (or C1), which is very favorable for stereoelectronic reasons! The 2-endo attack of F21′ has to happen from a less favorable direction on C2, and C2···F21′ is significantly larger than C2···F15. A 2-endo attack of F22′ could occur on a path that forms a smaller angle with the C2 p axis, but steric interactions with the 6-endo proton result in early hinderance (see Figure 12). Therefore, steric and stereoelectronic effects seem to favor the 2-exo attack and to disfavor the 2-endo attack, and this is in agreement with the almost exclusive formation of 2-exo products upon solvolysis of 2-exo *or* 2-endo derivatives.[53]

The 2-exo/2-endo differentiation during a nucleophilic attack on O-methylated camphor (**23**) is also reflected in the crystal packing of **23**-BF_4[54] (see supplementary material): the two nearest

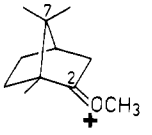

23

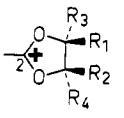

24

counterions seem to attack **23** with F15 from the exo side and with F17′ from the endo side (the numbering of the atoms is that from the Cambridge File;[55] the counterion with the primed atom labels is generated by the symmetry operation $x, y + 1, z$). Both attacks cannot take place along the optimal path: the endo attack is still hindered by the C5–C6 bridge (but less than in **20**, because **23** has a much weaker bridging), and the exo attack is even more hindered by the 7-syn methyl group (C11)! Solvolytic examinations[56] have shown that **23** yields a slight preference for the endo attack (exo:endo = 12:88). Without the C1 and the C7 methyl groups, the usual clear preference for the exo attack is observed: O-methylated norcamphor yields upon solvolysis exo and endo products in the ratio 96:4. The last example of a correlation between crystal packing and solvolysis behavior of carbocations that we would like to mention here is the case of the dioxolenium ions **24**.[57] The crystal structure of a typical example[58] (R_1, R_2 = $(CH_2)_3$; R_3, R_4 = H) with diastereotopic faces of the cationic carbon atom C2 reveals that the small steric hinderance allows for attack of the two nearest counterions on both sides of C2 practically perpendicular to the plane through C2 and its nearest neighbors (see supplementary material). Nevertheless, the cis attack is slightly hindered by the cyclopentane ring. Solvolysis studies of several other dioxolenium ions by King and Allbutt[59] have shown that the kinetically controlled attack on **24** leads preferentially to the trans product. Other crystal structures of dioxolenium ions[60] confirm this trend, although the spatial arrangement of the anions around the cation is of course influenced by normal packing forces, and it may be oversimplified to take only the interaction of a cationic carbon atom with the nearest negatively charged atom of a tetrahedral or octahedral counterion into account.[61] But at least in those cases, where extreme selectivities in solvolysis reactions are observed (7-norbornenyl and 2-norbornyl derivatives), the crystal packing of the salts reveals correlations with the solvolytic behavior.

Conclusions

The crystal structure of the 7-norbornenyl cation **7** shows a strong interaction between the empty orbital at C7 and the π electrons of the C2=C3 double bond and supports the earlier postulated concept of a bishomoaromatic stabilization of **7**. The qualitative resonance energy estimation based on the experimental structure and some calculated structures shows that even benzylic, tertiary carbocations are strongly stabilized by π participation of the C2=C3 double bond. The presence of static or dynamic disorder of the isomeric ions **7′** and **7″** can be excluded on the basis of electron and difference density maps of **7**, if it is assumed that **7′** and **7″** have structures similar to the corresponding neutral compounds. A similar type of disorder can be excluded for the earlier published 2-norbornyl cation **20**. The analysis of the crystal packing of the salts **7**-SbF_6 and **20**-Sb_2F_{11} and some other carbocation salts reveals a correlation between the arrangement of anions around the carbocations and the ratio of solvolysis products formed under kinetic control. Many apparently incompatible observations about the behavior of 7-norbornenyl or 2-norbornyl cations from NMR or solvolytic studies, which led formerly to controversies about the structures of the carbocations, can be explained without contradiction by analyzing the molecular and crystal structures of the carbocation salts.

Experimental Section

X-ray Crystal Structure Analysis of 7-SbF_6. The analysis was as follows: Enraf-Nonius CAD4 diffractometer, Mo Kα radiation, graphite monochromator, measurement at −80 °C, space group $P2_1/n$, a = 7.82 (1) Å, b = 15.03 (2) Å, c = 14.11 (1) Å, β = 104.37 (8)°, V = 1605 Å^3, ρ_{calc} = 1.792 g cm^{-3}, 3814 reflections up to ϑ = 28°, 2540 with $I > 3\sigma_I$. It was difficult to keep the orientation of the very slightly twinned crystal constant. Scans of the peak profile indicated a shoulder on some of the generally broad peaks (width less than 1°). For several dozen peaks, this shoulder fell into the background range, and consequently, the intensity of these peaks was far too small. These peaks were not sorted out, and this is considered to be the cause for the erroneous scale factor. The position of the Sb atom was determined with the Patterson option of SHELXS-86,[62] and all other non-hydrogen atoms were located in an automatic subsequent partial structure expansion. After several cycles of isotropic and anisotropic refinement with SHELX-76,[63] the hydrogen atoms at C1, C4, C5, C6, C72, C73, and C75 could be located by a difference Fourier map, but they were substituted by calculated H atoms and refined in the riding mode. Subsequent refinement of the non-hydrogen atoms ($w = 1/\sigma_I^2$) in the X-RAY system[64] gave R = 8.4% and R_w = 9.5%. The electron and difference density maps were generated with the XTAL[65] system. The crystallographic pictures were made with PLUTO[66] and ORTEP.[67] The difference density maps of the SbF_6 anion in the structure

(52) Reference 42, footnote 14.
(53) Erman, W. F. *Chemistry of the Monoterpenes*; Marcel Dekker: New York, 1985; Vol. B, pp 1067–1093.
(54) Montgomery, L. K.; Grendze, M. P.; Huffman, J. C. *J. Am. Chem. Soc.* **1987**, *109*, 4749–4750.
(55) Allen, F. H.; Kennard, O.; Taylor, R. *Acc. Chem. Res.* **1983**, *16*, 146–153.
(56) Traylor, T. G.; Perrin, C. L. *J. Am. Chem. Soc.* **1966**, *88*, 4934–4942. Nickon, A.; Lin, Y. *J. Am. Chem. Soc.* **1969**, *91*, 6861–6863.
(57) Review: Pindur, U.; Müller, J.; Flo, C.; Witzel, H. *Chem. Soc. Rev.* **1987**, *16*, 75–87.
(58) Paulsen, H.; Schüttpelz, E. *Chem. Ber.* **1979**, *112*, 3214–3220.
(59) King, J. F.; Allbutt, A. D. *Can. J. Chem.* **1970**, *48*, 1754–1769. King, J. F.; Allbutt, A. D. *Can. J. Chem.* **1969**, *47*, 1445–1459. King, J. F.; Allbutt, A. D. *Tetrahedron Lett.* **1967**, 49–54.
(60) (a) Paulsen, H.; Dammeyer, R. *Chem. Ber.* **1976**, *109*, 605–610. (b) Paulsen, H.; Dammeyer, R. *Chem. Ber.* **1973**, *106*, 2324–2332. (c) Paulsen, H.; Dammeyer, R. *Chem. Ber.* **1976**, *109*, 1837–1849.
(61) A more detailed analysis of these observations is in preparation.
(62) Sheldrick, G. SHELXS-86, program for the solution of crystal structures from diffraction data; University of Göttingen, 1986.
(63) Sheldrick, G. SHELX-76, program for crystal structure determination; University of Göttingen, 1976.
(64) The X-RAY system, Version of June 1972. Technical report TR-192, June 1972; Computer Science Center: University of Maryland.
(65) XTAL, Version 2.4; Hall, S. R., Stewart, J. M., eds.; University of Western Australia and University of Maryland: 1988.
(66) PLUTO88, plot package for the display of crystal and molecular structures; Cambridge Crystallographic Data Centre, University Chemical Laboratory: Cambridge, U.K.

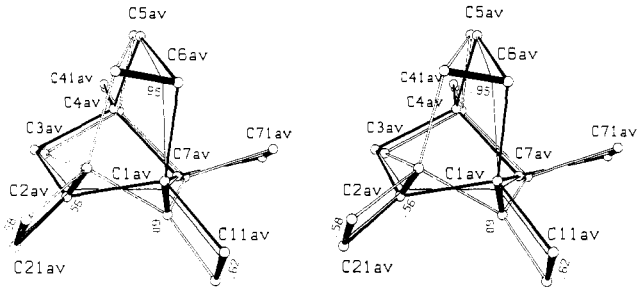

Figure 13. Stereo drawing of the superposition of 1,4,7-*anti*-trimethyl-2-methylenenorbornane (**21**) with 1,3-*endo*,4-trimethyl-2-methylenenorbornane (**22**) (medium–thick black and white bonds; structure, MM2(85)[23]). The structure generated by 3:1 averaging of corresponding positions of all carbon atoms is represented by thin bonds and atom labels with the appendix "av". The lines connecting each pair of corresponding atoms in **21** and **22** are represented by thick bars, and some of their lengths are given in angstroms.

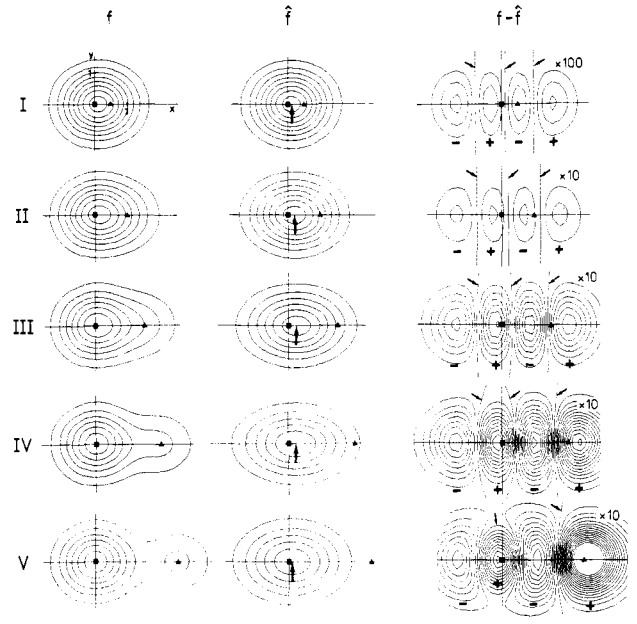

Figure 14. Adjustment[41] of three-dimensional anisotropic Gaussian density functions $\hat{f}$ (maxima: big arrows) on superpositions of two isotropic Gaussian density functions f (components: weights 0.75 and 0.25, maxima at ■ and ▲, equal temperature factors) by minimization of $\int(f-\hat{f})^2\,dV$. The functions f and $\hat{f}$ are normalized ($\int f\,dV = \int \hat{f}\,dV = 1$). The contour lines are drawn in a plane containing the symmetry axis (x) and have density distances of 0.02 for f and $\hat{f}$ and of 0.0002 (I) or 0.002 (II–V) for $f-\hat{f}$. The zero contours of $f-\hat{f}$ are marked by small arrows and the signs refer to the sign of $f-\hat{f}$. Distances of the maxima of the component functions of f (in length units) and $(\int(f-\hat{f})^2\,dV/\int f^2\,dV)^{0.5}$: I, 0.5, 0.5%; II, 1.0, 3.9%; III, 1.5, 11.8%; IV, 2.0, 22.7%; V, 2.5, 31.6%.

of **7**-SbF_6 (and also of the Sb_2F_{11} anion in the crystal structure of **20**-Sb_2F_{11}) reveal a slight orientational disorder of the SbF_6 units. In all cases, the Sb atoms are in the difference density maps surrounded by nearly symmetrical pairs or quadruplets of positive or negative peaks, which may indicate that the inclusion of high-order terms in the temperature factor of the Sb atoms could also be necessary for a satisfactory explanation of the F_{obs} maps. Separate thermal motion analyses[68] for the cations and anions in **7**-SbF_6 and **20**-Sb_2F_{11} suggest that the octahedral SbF_6 units can be treated as relative rigid groups, but the whole Sb_2F_{11} anion has a considerable flexibility. The root-mean-square differences of the mean-square displacement amplitudes between all pairs of atoms of the cations (in 10^{-4} Å^2: 54 for **7**, 95 for **20**) are about $2^{0.5}$ times the standard deviations of the experimental U values. The rigid-body model reproduces U values for both cations within the given (low) accuracy

(67) Johnson, C. K. ORTEP-II, thermal-ellipsoid plot program for crystal structure illustrations, Oak Ridge National Laboratory: Oak Ridge, TN, March 1976.

(68) Trueblood, K. N. THMA11, Version of 18 May 1987; University of California: Los Angeles, 90024.

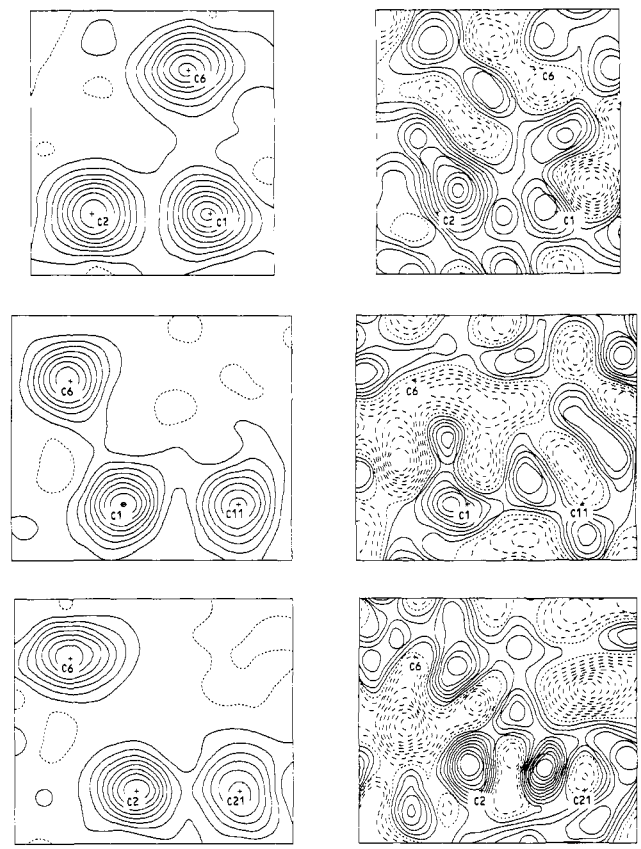

Figure 15. Electron density (left; F_{obs}; distance of the contour lines, 1 e/Å^3) and corresponding difference density maps (right; $F_{obs} - F_{calc}$; distances of the contour lines, 0.1 e/Å^3) of **20** (positive values, solid lines; negative, dashed; zero, dotted).

(roots of the eigenvalues of the **T** and **L** tensors: for **7**, 0.22 Å, 0.20 Å, 0.18 Å, 4.0°, 2.7°, 2.4°; for **20**, 0.22 Å, 0.15 Å, 0.09 Å, 5.0°, 3.3°, 2.5°; $\langle(U_{ij_{obs}} - U_{ij_{calc}})^2\rangle^{0.5}$ and $\langle(\sigma(U_{ij_{obs}}))^2\rangle^{0.5}$ in 10^{-4} Å^2: for **7**, 31 and 34; and for **20**, 48 and 79). All distances are not corrected for libration.

Note Added in Proof. The estimated resonance energies for **1** or **7** should not be compared with the isodesmic reaction energies in ref 14. Schleyer et al. found that the reaction involving the parent ion **1**

7-norbornyl cation + norbornene → **1** + norbornane

is exothermic with $\Delta H = -15$ kcal/mol, because the norbornene is in this reaction in its ground-state conformation. A better comparison would require the use of a bent norbornene with a structure similar to that of **1** on the left side of the above equation.

Acknowledgment. I thank Christoph von dem Bussche-Hünnefeld and Thomas Blatter for their great help with the synthesis of the precursors of **7**-SbF_6 during the summer term of 1987, Prof. Dr. R. M. Coates for submitting a procedure about the conversion of polycyclic alcohols into chlorides,[21] Prof. Dr. Paul von Ragué Schleyer for submitting a manuscript about ab initio calculations,[14] and Paul Seiler, Dr. W. Bernd Schweizer, and Prof. Dr. Volker Gramlich for their help during the measurements and evaluation of the X-ray data. The "Fonds der Chemischen Industrie" (Federal Republic of Germany) sponsored the work by the allocation of a "Dozentenstipendium". Financial support of the ETH is gratefully acknowledged.

Registry No. **7**, 123639-49-6; **7**-SbF_6, 123723-81-9.

Supplementary Material Available: Crystal packing diagram of **7**-SbF_6, tables listing the atomic coordinates and internal coordinates for **7**-SbF_6, data on the comparisons of **7** with other structures, and energy estimations, electron density maps, and stereodrawings for **23**-BF_4 and **24** (27 pages); tables of calculated and observed structures factors (20 pages). Ordering information is given on any current masthead page.